

LOOKING AT STARTING TRANSIENTS AND TONE COLORING OF THE BOWED STRING

Knut Guettler

Norwegian Academy of Music
P.O. Box 5190 Majorstuen, 0302 Oslo, Norway
knut.guettler@nmh.no

Abstract

The last decade has brought many answers to questions concerning bowed-string onsets and how tone color is controlled by the player. Also, new friction models have emerged, models that relate friction coefficients to contact temperature rather than to the relative velocity. This implies both starting transients and timbre to be considerably more influenced by the properties of the rosin than was earlier presumed. The present paper reviews recent findings in these fields.

Key words: *Bowed string, Music transient.*

Control of tone color during steady state

The four most basic parameters used by the player to control the tone color of a bowed instrument are

- (1) bowing “pressure” (i.e., the bow’s *force*, normal to the string)
- (2) bowing speed
- (3) bowing position on the string
- (4) tilting of the bow hair ribbon with respect to the string.

It has earlier been shown that the parameter “bowing pressure” (1) influences the spectral envelope by sharpening the Helmholtz corner each time it passes the bow¹. What has not been equally clear is whether this sharpening is related to the *absolute*, or *relative* bow force, the latter with respect to the area between the upper and lower limits for maintaining the Helmholtz motion with a given bow speed. These limits are outlining a wedge in the Schelleng diagram², where bowing position constitutes the abscissa. (See Figure 1.) The bow force limits in Schelleng’s diagram are based on the following two equations:

$$F_{\max} \doteq \frac{Zv_B}{(\mu_S - \mu_d)\beta}, \quad F_{\min} \doteq \frac{Z^2v_B}{2R(\mu_S - \mu_d)\beta^2}, \quad (1)$$

where Z = characteristic wave impedance; v_B = bow speed; μ_S and μ_d = static and dynamic friction coefficients, respectively; R = Resistance of bridge (the only string-termination loss);
 β = distance from bridge to point of excitation, relative to the total string length.

The rounding of the Helmholtz corner originates from bending stiffness, and internal and external losses with respect to the string, and cannot be derived from the equations above. However, the present paper suggests that tone color can be related to bow force *relative* to these limits. Higher partials are being emphasized when the *relative* bow force is increased. It follows that bow speed alone can influence timbre (lowering the speed emphasizes the higher partials), which has recently been proved empirically³. Figure 2 is a 3D version of Figure 1, introducing speed as the 3rd independent variable.

What is not immediately evident from Schelleng’s diagram, is whether the bow’s *position* (3), does carry any potential for changing the spectral envelope or roll-off frequency or not. However, the only spectral effect seen when changing the bowing position concerns the so-called “node frequencies”, or frequencies close to those. This may appear surprising, since in pizzicato the spectral envelope is indeed influenced by the excitation point, and most string players have “experienced” that “changing bowing position changes the tone color” in a similar fashion. On the other hand, players have hardly done so while keeping

parameters (1) and (2) constant, since that would quickly have brought them off the Helmholtz-mode regime. Figure 1 is based on the Schelleng diagram, but shaded in order to indicate that tone color gets brighter with increasing force rather than diminishing distance to the bridge.

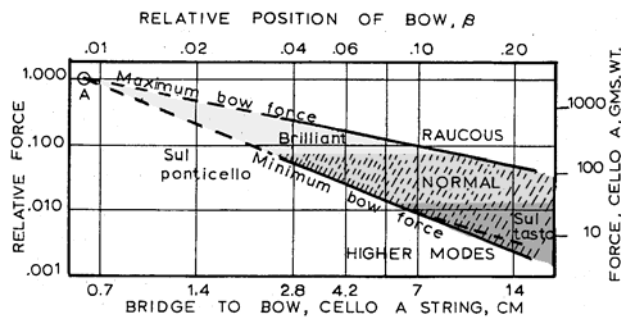


Figure 1: The Schelleng diagram (from JASA 1973). As function of relative bowing position, β , the wedge shows the bow force that will maintain Helmholtz motion for a given bow speed. The shaded sections, introduced by the present author, indicate three different tone-color characteristics: brilliant, neutral, and “sul tasto” (soft). These appear to be independent of bowing position.

Figure 2: 3D version of Schelleng’s diagram. The bow speed is now included. Lowering the bow speed while keeping other variables fixed, causes the tone color to become more sharp/brilliant.

Schelleng diagram including bow speed

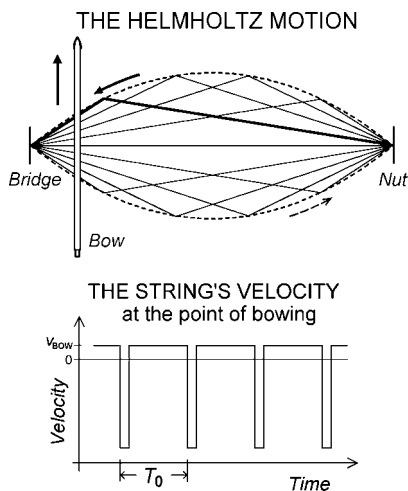
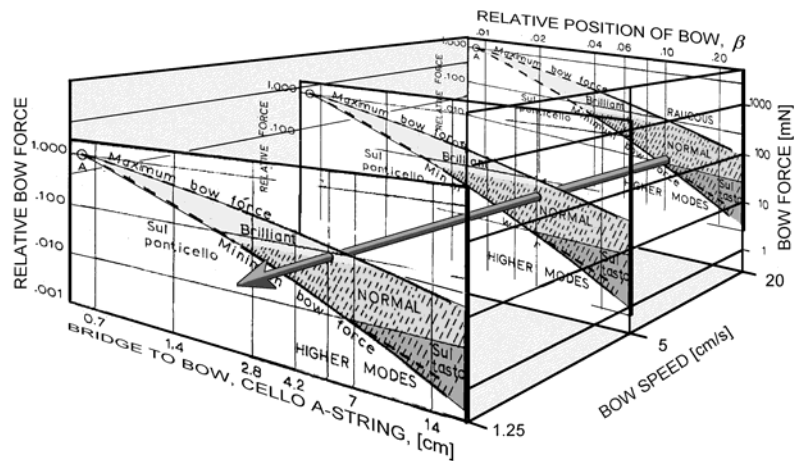


Figure 3: The Helmholtz motion of a bowed string. While oscillating in Helmholtz motion, the string generally describes two straight lines joined in a sharp rotating corner. During most of the period, the string follows the bow completely. The slip takes place when the corner is on the bridge side of the bow. The sharpness/rounding of the corner determines the sharpness/softness of the tone color.

Spectra of Pizzicato in two different positions

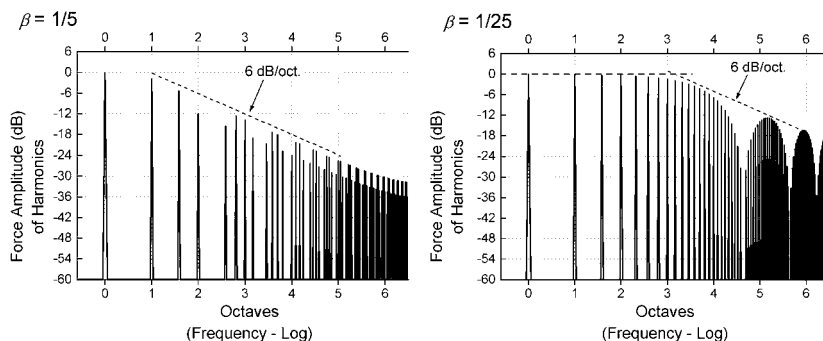


Figure 4: Pizzicato makes spectral lobes with widths dependent on the position of excitation. A wide first lobe hence causes the tone color to become more brilliant when plucking the string close to one of its ends.

When bowing a string in steady-state Helmholtz motion, the force acting on the bridge is principally describing a sawtooth wave, composed of a ramp, and a vertical edge that occurs every time the rotating Helmholtz corner is reflected at the bridge. The spectral slope of such a wave is -6 dB per octave. Had the bow been exciting the string at a point *irrational* to the total string length, the ramp would have been perfectly smooth. In practice the ramp is made up of a number of steps, the actual number depending on the bow's position. Spectrally, such steps cause certain partials to be weakened or suppressed. In the case of pizzicato, the force acting on the bridge describes a train of square pulses, the widths of which are determined by the time required for a string wave to propagate from the point of excitation to the bridge and back again. Also this waveform has a spectral slope of -6 dB/oct. However, unlike when the string is bowed, in pizzicato the spectrum also consists of *lobes* after the formula: *amplitude of harmonic* $n \propto \sin(n\pi\beta)/n\pi\beta$. This implies that when plucked near one of its ends the string will produce a wide first lobe with a number of partials holding amplitudes close to unity (see Figure 4). The tone will sound bright.

The brilliance or tone brightness of the bowed string can only be modified through shaping of the Helmholtz corner. When the string slips on the bow hair, a transitional interval occurs, where the relative speed between the bow and the string gradually reaches a maximum. A similar, but reversed situation occurs when the string is captured (see Figure 5). Had the transition been instantaneous, the Helmholtz corner would have been perfectly sharp, and the spectrum would display no roll-off frequency at the high end. In practice losses and bending stiffness round off the corner, while the bow, on the other hand, sharpens it every time it passes. The (relative) force determines how much.

The sharpness of this corner is for any practical measures independent of β , that is, independent of the time interval between release and capture. In the force signal, the string's accelerations at release and capture cannot be distinguished, as they are two sides of the same coin. When β changes, one *can*, however, see local variations in the (normalized) spectrum—particularly around the “node frequencies”, i.e., frequencies in the neighborhood of $f = nf_0/\beta$, where $f_0 =$ the fundamental frequency, and $n = 1, 2, 3$, etc—but no tendency towards brighter or softer tone color in general. See Figure 6, resulting from six simulations of a violin G-string.

Figure 5: Schematic plots of the string's velocity during the slip phase with two different bowing positions. Spectrum is determined by the relative *acceleration* at release and capture—not the time interval between these two steps. The force spectrum at the bridge is without lobes.

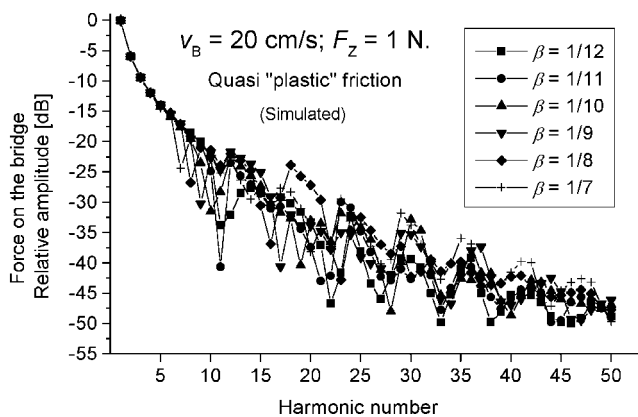
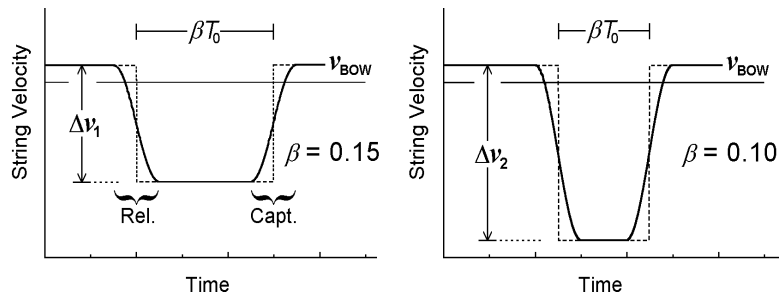


Figure 6: Simulated force spectra of violin G-string bowed at six different positions while keeping other bowing parameters fixed. In spite of local excursions around the “node frequencies” there is no trend towards greater brilliance as the relative bowing position (β) gets smaller.

An experiment was recently set up for the verification of bow speed as controlling parameter for tone color³. Here a bowing machine was used for controlling the bowing parameters. The result can be seen in Figure 7:

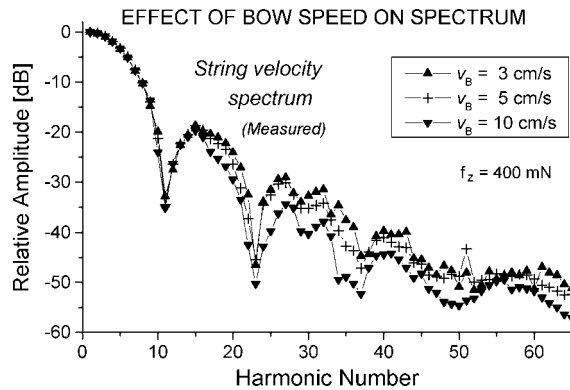


Figure 7: Spectra of an open violin D-string bowed with three different velocities (normalized to the amplitude of the 1st harmonic). As the velocity decreases, the relative energy of high partials increases.

When normalizing the amplitudes to zero dB for the first harmonic, a reduction of the speed from 10 to 3 cm/s gave an average increase of 5.2 dB for harmonics 16 to 65. It is particularly when the upper bow force limit is approached (by lowering the bow speed—see Eq. 1) that such a spectral change takes place. The spectral difference between bow speeds of 30 and 10 cm/s produced only an average difference of 0.2 dB for the same range of harmonics. The underlying physics for these changes in tone color can be traced back to simple stability requirements. Regard Figure 8, which describes “ideal” Helmholtz conditions with a simple friction model: In steady state, for a given β , bow speed, and bow force, the friction will alternate between Q_s (quiescence during stick) and Q_d (quiescence during slip). Over one period (T_0), these two conditions will occupy $T_0(1-\beta)$, and $T_0\beta$, respectively. Disregarding all losses, Q_s and Q_d must be balanced to the same force level if the string shall be driven in steady state and no net amount of work shall be done in the course of a period⁴. The interval between Q_d and Q_s projected onto the abscissa is equal to v_B/β . If we reduce the bow speed, v_B , this distance becomes smaller, which implies that Q_d and Q_s have to move up to higher force values in order to maintain alignment while still being placed on the friction curve (see Q_d' and Q_s' of Figure 8). This increase in friction force seems to be the main reason why the Helmholtz corner gets more sharpened and the tone brighter when the bow speed is reduced, also for more realistic friction models. (Figure 2 of the paper “Applications of the Bluestein filter...”, printed elsewhere in these proceedings, gives an example of velocity measurements of a violin D-string bowed with different bow speeds.)

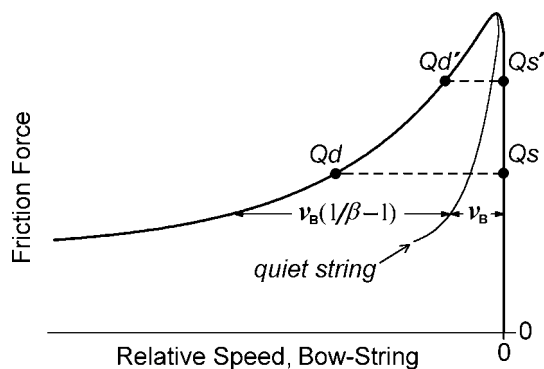


Figure 8: Friction curve and stability requirements under simplified Helmholtz conditions. During stick, the relative speed between bow and string is zero, while it is v_B/β during slip. In both cases the friction must take the same force value in order not to generate net work over the steady-state period. This implies that the friction force must *increase* as v_B —and thus the interval between Q_d and Q_s —becomes smaller.

The effect of bow-hair tilting has been a theme of discussion among string players. While all violinists and violists normally play with the bow-hair ribbon tilted with respect to the string, some cellists and even more double bassists play with the hair flat (usually with the conviction that “it provides better friction”). On a violin, the full width of the bow hair (ca 8 mm) occupy at least 2.4% of the string length when put flat on, while on the double bass the comparable figure is about one half of that. It is not difficult to imagine that some short-wavelength filtering effect might take place. The exact

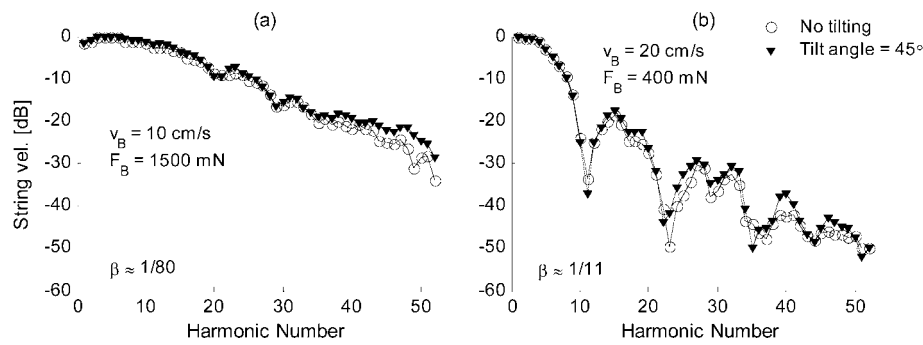


Figure 9: Effect of bow-hair tilting on the string spectrum (after Schoonderwaldt et al. 2003).

mechanism has yet to be revealed, however, but it has been confirmed that reducing the width of the touching bow-hair ribbon in fact does encourage higher partials, and bow-hair tilting even more so (particularly when bowed near the bridge), although the audible effects are moderate⁵.

Based on the information discussed above and confirming simulations, it is possible to present the following table, which gives a general overview.

Table 1: Overview over steady-state spectral effects when changing one bowing parameter (only):

| Parameter value <i>increased</i>: | Effect on tone color (spectral profile): |
|--|--|
| Bow force (“bow pressure”) | Increased sharpness/brilliance |
| Bow speed | Decreased sharpness/brilliance |
| Relative bowing position (β) | Only local deviations – No general tendency |
| Tilting of bow-hair ribbon with respect to the string (only if tilted the correct way, i.e., toward the fingerboard). | Increased sharpness/brilliance (moderate effect only) |
| Width of bow-hair ribbon | Decreased sharpness/brilliance (moderate effect only) |
| Length of string (with constant stiffness, and impedance—but the fundamental frequency decreasing) | Increased sharpness/brilliance (relative to the fundamental frequency) |
| *Wave resistance (mass <i>and</i> tension) of the string [i.e., $Z = \sqrt{(T\delta)}$, where T = tension, and δ = mass per unit length] while keeping the tuning fixed, i.e., holding T/δ constant. | Decreased sharpness/brilliance [Although: increased wave resistance permits a higher limiting bow force—see Eq. (1)—which gives comparatively higher sharpness/brilliance when the string’s bending stiffness is kept unaltered.] |
| *Loss at string terminations | Decreased sharpness/brilliance (notice from Eq. 1 that reducing R increases F_{\max} , and thus decreases the <i>relative</i> bow force) |
| *Bending stiffness of string | Decreased sharpness/brilliance It also increases chances for “pitch flattening”. When playing a thick string in high positions, the relative bending stiffness increases due to the greater proportion of corner rounding. |
| *Softness of rosin | Increased sharpness/brilliance (giving the an effect comparable to increased bow force). “Pitch flattening” may increase. |

* These parameters are not normally subjected to changes during a performance, but are listed here for completeness.

The onset transient—creation of the Helmholtz motion

During the “attack” (or “tone onset” as one might prefer to label it) the rotating Helmholtz corner has to be constructed. This presupposes a gradual buildup of waves on each side of the bow. Figure 10 shows this principle of development: During the onset transient the high impedance bow pretty much acts like an isolator between waves rotating on either side. For a bow moving upwards the task is to produce waves that return from the bridge and nut with *descending* and *ascending* steps, respectively (see “steady state”, lower panel in Figure 10). On the bridge side, descending steps will come naturally as reflections of the first slip. On the nut side, reflection of the first slip will arrive at a time $T_0(1-\beta)$ after the first release, then again at the time $2T_0(1-\beta)$, etc. In order to develop *ascending* steps, reflections of the first release must be smaller in amplitude than that of the second release, and so on. This could either happen through acceleration of the bow (the flyback velocity increasing), or through losses at the reflection points, causing pulses to fade at each reflection. In practice the latter would only be sufficient if β is small so that many reflections take place before the sequence repeats itself.

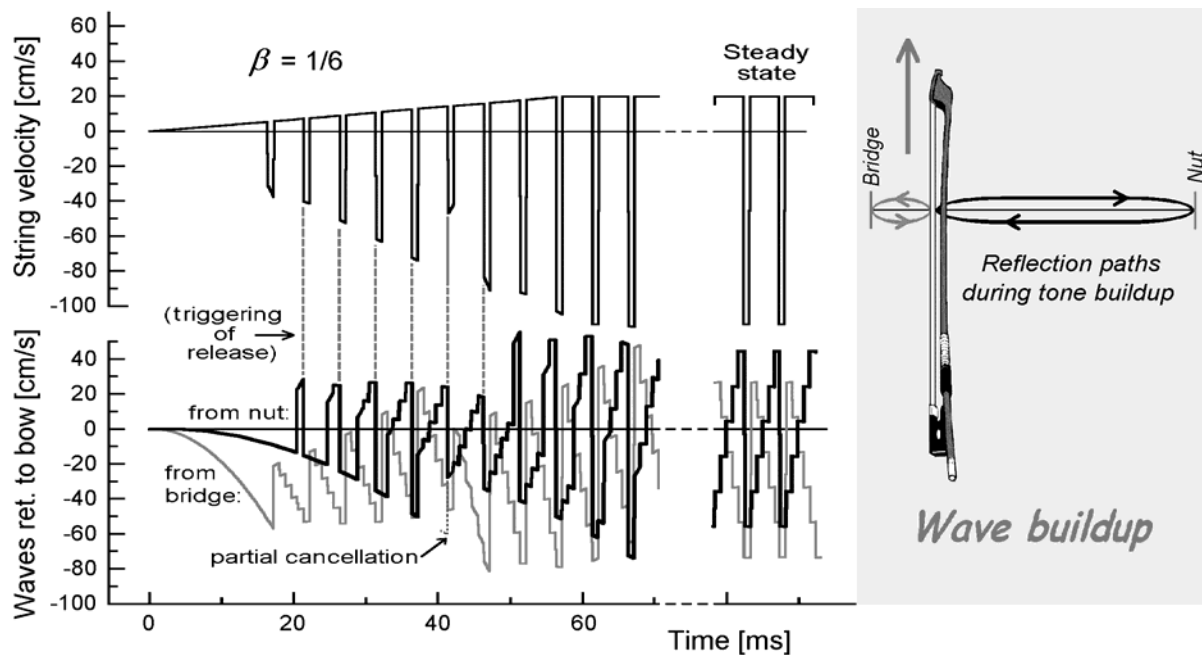


Figure 10: Wave buildup during a bowed tone onset (simulated). The reflection pattern is different on each side of the bow (see lower left panel). While the waves returning to the bow from the bridge obtain a correct pattern directly after the first slip (compare to the steady-state situation, where *descending* steps are seen), the waves on the nut side require a gradual circular overlap to achieve the correct Helmholtz pattern of *ascending* steps in steady state.

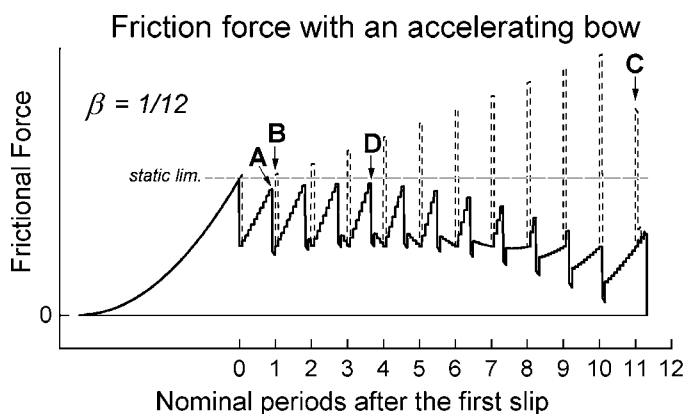


Figure 11: Friction force during an attack with regular stick/slip triggering from the start—the bow given a constant acceleration. There are four crucial points of time, where friction force must stay below (A and D), or surpass (B and C) the limiting static friction force in order to develop triggering regularly.

In the case of the (constantly) accelerating bow, there are four obstacles that potentially could destroy regular stick/slip triggering to follow the first slip (labeled A through D in Figure 11). If accelerating to much, the peak at A [situated at the time $T_0(1-\beta)$ after the first release] would cause a premature slip. At B [situated at the time T_0 after the first release] the returning waves must oppose the bow's movement enough to cause a slip, i.e., the bow velocity minus the sum of all returning waves, times the impulse impedance of the string surface, (short dashes in Figure 11) must surpass the limiting static friction force. This requires acceleration to be *above* a certain value. The same is true at C [situated at a time near $T_0(1/\beta - 1)$ after the first release]. Had the bow been starting with a constant *speed* "switched on", the string would only have been released at this point if β was small. If not, the pulse originating at the first slip would not have been sufficiently reduced to avoid canceling of release here (see reduction of flyback velocity at the 6th, and force at the 12th slip of Figures 10 and 11, respectively). If the bow starts with acceleration, however, a fourth obstruction will be present as a force peak at the time near $T_0(1-\beta)/(3\beta)$ after the first release (labeled D in Figure 11). Similar to the peak at A, this peak could easily cause a premature slip.

When using a simple resistive bowed-string model like Raman⁶ and Schelleng did, it is possible to calculate the range of accelerations that will provide regular stick/slip triggering⁷. For small β the peaks at B and D restrict the range of "successful" accelerations more than the ones at A and C. For large β , peaks at A and C would be representing the limiting factors. For more complicated string models this pattern can be recognized, although probably not possible to calculate.

Figure 12 shows a set of 33000 simulations using more realistic string and friction models. Each pixel represents a unique combination of the bowing parameters acceleration and force. The color of the pixel indicates the number of nominal periods elapsing before Helmholtz triggering occurs. The string simulated is a high-gauge violin G-string (with torsion, quasi-plastic friction model, etc., described in ref⁷). The area labeled (1) represents *prolonged periods* ("failing" at B or C), which gives a "choked" or "creaky" sound. Area (2) indicates "perfect attacks" (i.e., periodic triggering from the start), while (3) represents *multiple slips* ("failing" at A or D), implying a "loose" or "scratchy" transient sound.

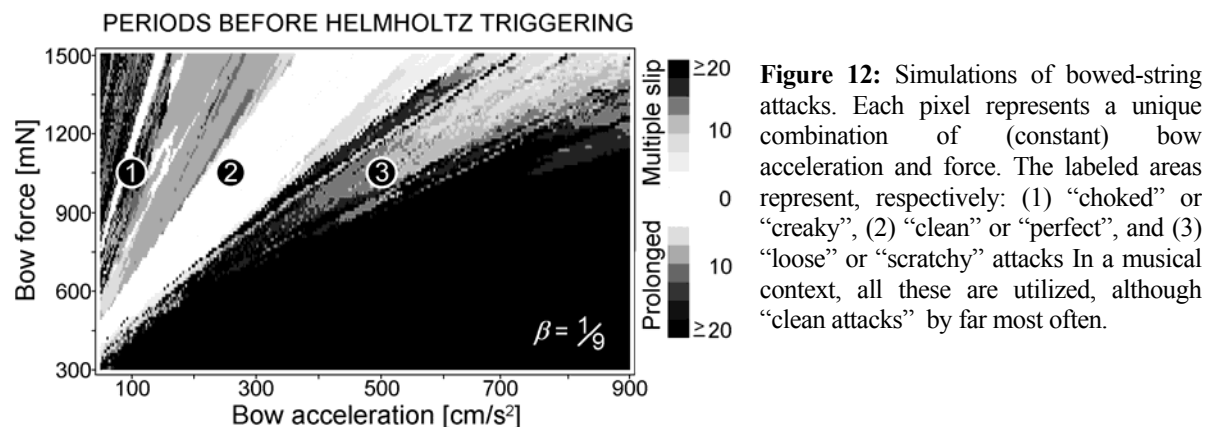


Figure 12: Simulations of bowed-string attacks. Each pixel represents a unique combination of (constant) bow acceleration and force. The labeled areas represent, respectively: (1) "choked" or "creaky", (2) "clean" or "perfect", and (3) "loose" or "scratchy" attacks. In a musical context, all these are utilized, although "clean attacks" by far most often.

The creation of the Helmholtz motion has through listening tests been subjected to study in terms of musical preference⁸. For violin onsets to be judged as "acceptable" in a musically neutral context, no more than 90 milliseconds should elapse before establishing the Helmholtz slip/stick pattern when extra string slips are present (the sound being "loose/scratchy"), and no more than 50 ms when slipping intervals are longer than the nominal fundamental period (the sound being "choked/creaky"). As we see from Figure 12, these effects take place when the bow's initial acceleration is too small or high for the given bow force, respectively. In this study two professional violinists played excerpts of musical pieces of different character while the string movement was recorded and later analyzed. The musicians were not aware of the purpose of the test. It turned out that more than 50% of a body of 1694 attacks could be categorized as "perfect", while musical style to a large degree determined

whether the remaining part would fall into category (1) or (3). Taken into consideration that the requirements of bow acceleration vary with: frequency, string properties, β , and dynamics—so that each tone played has to be given individual bowing parameters—it is quite impressive how well accomplished players master this challenge.

Figure 13 shows spectrograms of the three categories of bowed attacks. The recordings were done with a special electret microphone inside the violin, with a bowing machine producing attacks on the open G-string (G_3 at 196 Hz). This special arrangement favors to some degree the fundamental, which would otherwise be poorly radiated due to the small size of the violin. Some quite characteristic features are seen in each panel. The “creaky/choked” signal starts with a single string-flyback snap, which is unrealistic for classical playing, but interesting from the point of view that it emphasizes natural resonances of the instrument. After that, the actual tone building starts, slowly emerging from massive noise. The player can relatively easily determine the swiftness with which this transition takes place, which makes such onsets suitable for loud harsh, or percussive attacks, etc. Characteristic of the “perfect” signal is that all partials, including the fundamental frequency, are immediately apparent. Well-performed bow changes show comparable features. The noise seen here, is mostly sliding noise during the (regular) slipping intervals. The spectrum of this noise is to a large extent reflecting the resonance profile of the instrument, which will be audible for most tones played. One other typical attribute is a slight (mostly inaudible) pitch flattening during the initial part of the attack. The “loose/scratchy” signal shows in the present recording two slipping intervals per nominal period for about 350 ms. Twin slips oppose generation of the fundamental frequency and some other partials, dependent on the time interval between them. Extra slips naturally produce extra noise, which can be noticed in the spectrogram. This kind of attack is often used for “dreamy” or “transparent” musical characterization.

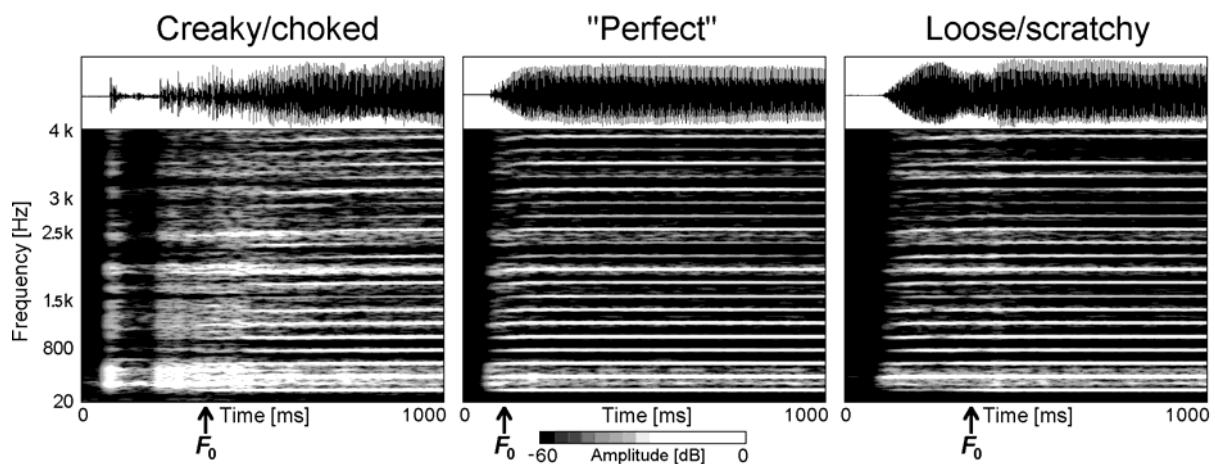


Figure 13: Spectrograms of three violin attacks. Notice the prevailing noise present in the left panel (creaky/choked). The middle panel (“perfect”) gives the cleanest spectrum, with quick buildup of all partials, including the first harmonic (F_0). In the right panel (loose/scratchy) the string slips twice per nominal period for about 350 ms, and the buildup of partials is comparatively slow and deficient. In both the rightmost and the leftmost panels F_0 appears only after a substantial delay. The stochastic energy in the frequency range 250-550, and around 2400 Hz, present in all panels, reflects normal slipping noise emphasized by major resonances of the instrument.

To sum up: through acceleration the player has a tool for coloring the bowed attack without substantially changing the dynamics. This technique, however, is only part of the player’s palette, since many bow strokes are started with the bow “off the string”, either approaching the string slowly (for gentle attacks) or quickly (for spiccato or ricochet, with the bow bouncing on and off the string). In the first case, multiple slips will usually take place, but, to some extent be masked by a rapidly developing Helmholtz triggering. Because double or multiple slips usually fade out as function of frequency and damping,

“loose/scratchy” attacks tend to last more shortly on high-pitched instruments. For this reason cellists and double bass players usually start their bow strokes nearer to the string, even for gentle attacks. Bouncing-bow techniques can produce clean (“perfect”) attacks, as has been shown by Guettler and Askenfelt^{9,10}, but this requires precision and quality both of the player and the bow itself. In general, string players consciously select the starting points on the bow-hair ribbon to shape the attack in accordance with the musical demands, taking advantage of bow’s dynamic properties for controlling the bow force envelope. Differences in tone color between up bow and down bow has been claimed, but never convincingly documented.

New friction models—impact on tone color

Traditionally, two friction models have dominated earlier discussions on the bowed string: the exponential and the hyperbolic friction-coefficient curves, both functions of the relative velocity between the bow hair and the string’s surface. Their respective equations can be given the following forms:

$$\mu_{EXP} = c_1 \exp\left(\frac{-V}{v_1}\right) + c_2 \exp\left(\frac{-V}{v_2}\right) + c_3. \quad (2)$$

and

$$\mu_{HYP} = \frac{c_1}{V + c_2} + c_3, \quad (3)$$

where V is relative velocity; c_n and v_n are constants.

While Eq.(2) gives the most precise fit for (empiric) steady-state sliding, Eq.(3) has the advantage that in bowed-string simulation it can be solved directly when V without friction is known, which implies faster computation. However, experiments carried out by Smith and Woodhouse¹¹ suggest that *temperature* rather than relative velocity determines the friction coefficient. Their “plastic-friction model” can be expressed as:

$$\mu_{PLAST} = \frac{A k_y(Temp)}{N} \text{sgn}(V), \quad (4)$$

where A is contact area; N is normal force; $Temp$ is temperature;

$k_y(Temp)$ is shear yield stress (function of temperature).

This expression, in which the shear yield stress is related to dissipation, temperature flux, and plastic properties of the rosin, has to be solved through a number of iterations. With appropriate parameters, however, it appears to yield a quite good approximation of the dynamic properties observed, except for a couple of shortcomings: It gives unrealistically high coefficients during the initial slip in starting transients (due to inadequate heating), and unrealistically high temperatures for high bowing speeds¹².

Other models that have been proposed, take into consideration the possibility of bristle-like properties of the rosin¹³. None of these suggest the presence of adhesion, which, in this author’s opinion, is likely to be an important feature of at least some of the rosins commercially available. One major difference between the plastic friction models and their predecessors, is that the plastic model prevents the discontinuities produced by the exponential and hyperbolic models when the relative velocity jumps directly from zero (in combination with the limiting static friction force during stick), to a high velocity (in combination with a low sliding-friction value at release). That is, a jump from the apex of the friction curve to the coordinate where the string’s load line intersects with its tail. Such discontinuous behavior brings forth high-partial energy that would never be observed in real strings. With the temperature-related plastic model, this transition is bound to happen gradually, even for strings that are perfectly flexible. Figure 14 shows simulations with two quasi-plastic models, their only difference being the time constant, which controls how fast changes of friction coefficient happen. The panels show spectra and frictional hysteresis of a string in steady-state Helmholtz motion, all bowing parameters fixed.

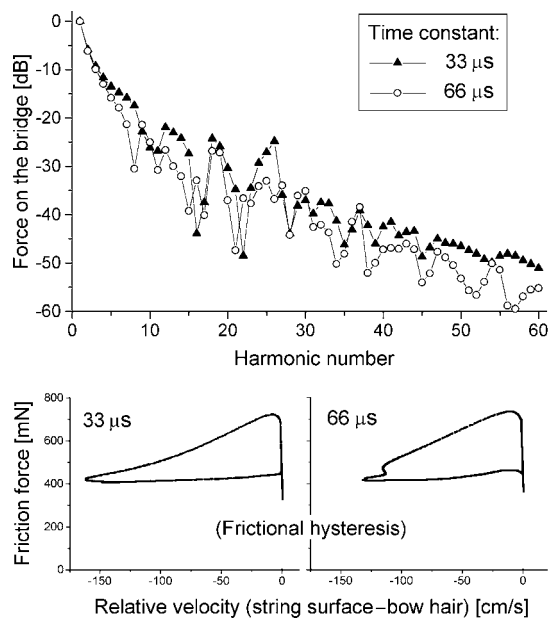


Figure 14: Comparison of friction models with two different (temperature-flux) time constants. Simulation of high-gauge violin G-string played at 196 Hz.

Upper panel: Spectra of force on the bridge during steady state (bowing parameters fixed). Notice how the energy of higher partials is reduced when the time constant of the friction model is increased.

Lower panels: Trajectories of friction force vs. relative velocity. The maximum speed during slip decreases as the time constant increases. This forces the slipping period to occupy a greater interval. A slight prolongation of the fundamental period was also observed. (Noise generation not included in this simulation.)

References

- ¹ Cremer, L. (1972 and 1973) "The influence of 'bow pressure' on the movement of a bowed string. Part I and II". *NL. Catgut Acoust. Soc.* #18, 13-19 and #19, 21-25.
- ² Schelleng, J. C. (1973) "The bowed string and the player". *J. Acoust. Soc. Amer.* 53(1), 26-41.
- ³ Guettler, K., Schoonderwaldt, E. and Askenfelt, A., (2003) "Bow speed or bowing position—which one influences the spectrum the most?" *Proceedings of the Stockholm Music Acoustics Conference (SMAC'03)* Vol. I, 67-70.
- ⁴ Weinreich, G., and Caussé, R., (1991) "Elementary stability considerations for bowed-string motion". *Journal of the Acoustical Society of America*, 89(2), 887-895.
- ⁵ Schoonderwaldt, E., Guettler, K., and Askenfelt, A., (2003) "Effect of the bow-hair width on the violin spectrum" *Proceedings of the Stockholm Music Acoustics Conference (SMAC'03)* Vol. I, 91-94.
- ⁶ Raman, C. V., (1918) "On the mechanical theory of the vibrations of bowed strings and of musical instruments of the violin family, with experimental verification of the results. Part I". *Indian Assoc. for the Cultivation of Science, Bull* 15, pp 1-158.
- ⁷ Guettler, K. (2002) "On the creation of the Helmholtz motion in bowed strings", *Acta Acustica/Acustica* Vol. 88, 970-985.
- ⁸ Guettler, K., & Askenfelt, A. (1997). "Acceptance limits for the duration of pre-Helmholtz transients in bowed string attacks". *Journal of the Acoustical Society of America*, 101(5) Pt 1, 2903-2913.
- ⁹ Guettler, K. and Askenfelt, A. (1998). On the kinematics of spiccato and ricochet bowing. *Catgut Acoustical Society Journal*, 3(6) Ser. 2, 9-15.
- ¹⁰ Askenfelt, A., and Guettler, K. (1998) "The bouncing bow – An experimental study" *CASJ* Vol. 3, No 6 (II), 3-8.
- ¹¹ Smith, J. H., and Woodhouse, J., (2000) "The tribology of rosin", *J. Mech. Phys. Solids*, 48, 1633-1681.
- ¹² Galuzzo, P. M., and Woodhouse, J., (2003) "Experiments with an automatic bowing machine", *Proceedings of the Stockholm Music Acoustics Conference (SMAC'03)* Vol. I, 55-58.
- ¹³ Serafin, S., et al. (2003) "Bowed string simulation using an elasto-plastic friction model" *Proceedings of the Stockholm Music Acoustics Conference (SMAC'03)* Vol. I, 95-98.